Influence of Shale Gas Components on Jet Diffusion Flame

Liu Shuai[a,*] Wang Zhong[b] Zhao Yang[c] Li Ruina Qu Lei

Jiangsu University, School of Automobile and Traffic Engineering, Zhenjiang 212013,China

[a]lstcls@163.com [b]422629217@qq.com [c]171553404@qq.com

Key words: Shale gas; component; jet diffusion flame; computational fluid mechanics; methane

Abstract: Effect of different shale gas components on jet diffusion flame were studied using mathematical method in this paper. Changes of OH free radical in jet diffusion flame of two different shale gas components were researched, and the impacts of shale gas composition changes on mass fraction of methane, combustion velocity and temperature fields were also discussed compared with vehicle compression natural gas jet diffusion flames. The results show that, in process of shale gas diffusion combustion, OH free radical mainly in outer flame, higher concentration of OH free radicals produced by the combustion of shale gas with higher mass fraction of methane at the top of the flame; in the region the flame height is in the range of 0~3cm, mass fraction of methane is higher, methane consumption is fastest, and combustion is most intense; compared with shale gas with methane mass fraction of 62.9% and vehicle compression natural gas with methane mass fraction of 87.36%, shale gas with methane mass fraction of 93.5% has the highest Combustion temperature and the fastest combustion speed.

Introduction

Shale gas refers to exist in organic-rich shales and dissection, and mainly in the form of adsorption or free state, is an unconventional natural gas, composed mainly of methane. China is rich in shale gas resources, according to the Energy Information Administration's forecast, the reserves of global shale gas are $456\times10^{12}\sim716\times10^{12}m^3$, shale gas resources in China reaches $100\times10^{12}\sim144.4\times10^{12}m^3$, accounts for about 20 percent of the world's total reserves[1]. Due to the difference accumulation mechanism of shale gas, shale gas composition changes largely in the different regions, change interval of methane is 46.5%～99.8%[2~4].

Around the jet diffusion flames of natural gas and other gaseous fuel, domestic and foreign scholars have conducted researches. Zhang Yongming and Fang Jun[5] of University of Science and Technology of China, who used jet burner to study jet diffusion flame of Methane in the low pressure test chamber, when the mass flow of fuel increases, flame temperature and flame radiation heat increased. Zhao Zhenxing[6] of Xi'an Jiaotong University, who used different structure of burner to study ignition characteristics and combustion stability of gas, when inside diameter less than 8mm of burner, combustion stability decreased, when the concentration of hydrogen increased, combustion stability of gas increased. Research Status shows that, when the components of gas changed, the flame structure of jet diffusion combustion was differences, the component of shale gas in different parts was large differences. Necessary around the impact the component of shale gas changes research.

According to China's two regions of shale gas abundant rich reserves, used Non-premixed combustion model of FLUENT6.3, studied the impact of jet diffusion flame when the component of shale gas changed. Analysis of the changes of combustion temperature, velocity and mass fraction of reactants and products, explored the impact of the burner temperature of the central axis, speed

and distribution of the material. When flame height was different, studied the law of temperature and velocity and distribution of material.

Gas Components and Programs

China's shale gas reserves are mainly concentrated in two regions, Changning County of Sichuan Province and its surrounding areas, and Zhaotong of Yunnan Province and its surrounding areas[7]. Because there are some differences between the geological structure and the mechanism of accumulation, there is a big difference between the two areas of component of shale gas. The volume fraction of the shale gas of C_1 ~ C_4 hydrocarbons in Changning is 96.7%、1.2%、0.1%、0%, the volume fraction of the shale gas of C_1~C_4 hydrocarbons in Zhaotong is 78.9%、12.6%、4.9%、0.76%. Based on the conversion equation between mass fraction and volume fraction, we can get the mass fraction of each alkane gases of shale gas, conversion equation is as follows,

$$g_i = \frac{r_i m_i}{\Sigma r_i m_i} \times 100 \tag{1}$$

Shale gas can be considered an unconventional natural gas, based on the relevant national standards of CNG, determine the representative gas component of CNG. In order to study the difference of diffusion flame jet between shale gas and conventional gas diffusion, studied the conventional gas diffusion combustion jet.

Table1 shows the different shale gas and CNG each alkanes gas mass fraction. As shown in Table1, program1 representative of Changning district shale gas, program2 representative of Zhaotong district shale gas, program 3 representative of CNG.

Tab.1 The Mass Fraction of Each Component in Different Options

Program	Methane	Ethane	Propane	Butane	Alkanes total amount of gas
1	0.935	0.022	0.003	0	0.96
2	0.629	0.188	0.107	0.022	0.946
3	0.874	0.043	0.017	0.015	0.949

Mathematical Model and Mesh

Mathematical Model

Flow model uses the standard k-ε model, it applies to simulate turbulent flow in the pipe and channel. Standard k-ε model is a semi-empirical formula, it mainly based on the turbulent kinetic energy and diffusivity. k equation is the exact equation, ε equation derived from the empirical formula. Equation is as follows,

Turbulent kinetic energy equation,

$$\frac{\partial(\rho k)}{\partial t} + \frac{\partial}{\partial x_j}\left(\rho \overline{u_j} k\right) = -\frac{\partial}{\partial x_j}\left[\left(\mu + \frac{\mu_t}{\sigma_k}\right)\frac{\partial k}{\partial x_j}\right] + \mu_t \frac{\partial \overline{u_j}}{\partial x_i}\left(\frac{\partial \overline{u_j}}{\partial x_i} + \frac{\partial \overline{u_i}}{\partial x_j}\right) - \rho\varepsilon \tag{2}$$

Turbulent kinetic energy dissipation rate equation,

$$\frac{\partial(\rho \varepsilon)}{\partial t} + \frac{\partial}{\partial x_j}\left(\rho \overline{u_j} \varepsilon\right) = -\frac{\partial}{\partial x_j}\left[\left(\mu + \frac{\mu_t}{\sigma_\varepsilon}\right)\frac{\partial \varepsilon}{\partial x_j}\right] + C_1 \frac{\varepsilon}{K} \mu_t \frac{\partial \overline{u_j}}{\partial x_i}\left(\frac{\partial \overline{u_j}}{\partial x_i} + \frac{\partial \overline{u_i}}{\partial x_j}\right) - C_2 \frac{\varepsilon^2}{k} \tag{3}$$

Turbulent viscosity coefficient $\mu = \rho C_\mu k^2 / \varepsilon$.

This paper uses non-premixed combustion model to simulate, this model is not necessary to solve each component of the transport equation, Solution one or two conserved scalar transport

equation, according to the forecast of the mixture fraction distribution, derive the concentration of each component. By solving the transient distribution of mixture fraction f, we determine the chemical properties of quick response of the fluid, use the probability density function PDF to consider the effect of turbulence.

Radiation model uses the P-1 radiation model, this model has the following two equations,

Radiation equation of qr heat flow,

$$q_r = -\Gamma \nabla G \tag{4}$$

Transport equation of G incident radiation,

$$\nabla(\Gamma \nabla G) - \alpha G + 4\alpha\sigma T^4 = S_G \tag{5}$$

Among them, Γ —Parameters introduced

α —Absorption coefficient

σ s—Scattering coefficient

C—Linear anisotropic phase function coefficient

σ —Stephen - Boltzmann constant

SG—User-defined radiological

Meshing

Figure 1 is a diagram burner mesh. As can be seen from Figure 1, the structure of combustion model is cylinder The radius model is 3.6cm, Height is 7cm, the gas outlet radius of combustion model is 0. 36cm, the air outlet radius is 0.55cm, the gas outlet height is 0.36cm. Using tetrahedral mesh model to divide combustion model, encrypt grid at the gas outlet.

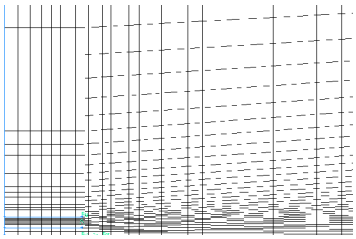

Fig.1 Partial Enlarged View of the Grid

Jet Diffusion Flame Analysis

The Distribution of OH Radicals and Methane Mass Fraction

Chain propagation of radical initiator and chain initiation reaction are dynamic of flame propagation, the concentration of free radicals plays an important role in the diffusion combustion, is an important indicator of the stability of the flame. Changes in the concentration of OH group is most evident in the combustion, combustion rate is closely related to the concentration of the OH groups of the flame[8]. Figure 2 shows the three scenarios jet diffusion combustion, concentration distribution field of OH radical in the flames. As can be seen from Figure 9, when the gas outlet diameter is 0.72cm, the exit velocity is 11.4cm/s, OH radicals concentrated in the outer region of the diffusion flame, external flame zone gas mixes well with air, combustion reaction focus, the reaction rate is faster, the combustion temperature is high, option one in shale gas combustion, the most concentrated area of focus at the top of the flame OH group, resulting in the combustion temperature is higher and flame speed is faster than other fuels, when option two and option three are burning, concentration distribution of OH radical looks like option one, OH group concentration of option three is greater than option two.

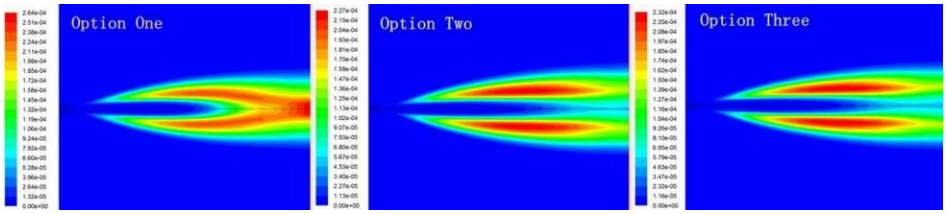

Fig.2 Distribution of OH Radicals in Diffusion Flames

Figure 3 shows when three options are burning, the distribution of the mass fraction of methane gas along the axis. As can be seen from Figure 3, when the gas outlet diameter is 0.72cm, outlet speed is 11.4cm/s, the axial distance is in the range of 0~0.25cm, methane mass fraction of three programs remained unchanged, indicate that the area is diverging section of gas, not sufficiently mixed with air, gas is not burning, the axial distance is in the range of 0.25~1.5cm, gas is from the diverging section into the larger area, rapid mixing of methane and air, combustion reaction speed is fast, the mass fraction of methane along the central axis is decreases rapidly, comparison of the three scenarios of mass fraction of methane combustion rate of decline can be seen, the mass fraction of methane combustion fastest decline in the option one, is showen that combustion speed is fastest in the option one, the mass fraction of methane is slowest decline in the option two, combustion speed is slow, when the axial distance is 3cm, the mass fraction of methane of three programs approaches zero, along the central axis of the basic burn methane.

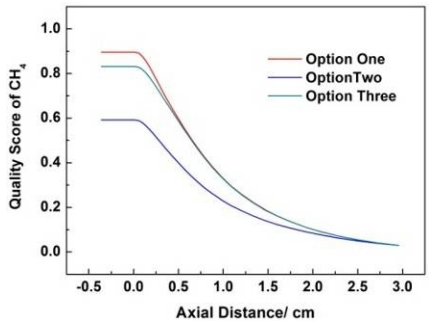

Fig.3 Methane Mass Fraction Distribution Along the Central Axis

Burning Velocity Field

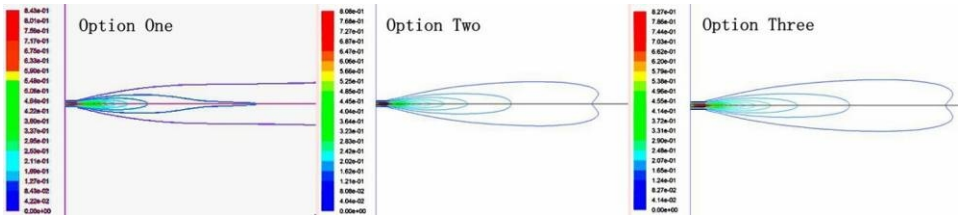

Fig.4 Combustion Velocity Contours Distribution

Figure 4 shows the velocity contours of three scenarios burning jet fuel gas diffusion distribution. As can be seen from Figure 4, when the gas outlet diameter is 0.72cm, outlet speed is 11.4cm/s, combustion velocity of three scenarios of gas vents is distribution, combustion velocity of option two and option three is similar, top convergence that looks like oval spread out, at the top of the outer air stream depression, heart-shaped distribution, combustion rate similar shows gas and air mixing speed close both two programs, combustion speed of gas is be oval distribution in the vicinity of the outlet in option one, outer is no convergence, be open distribution, comparing the contours of combustion velocity of the three options can be seen that, the gas and air mixture speed is slow in the option three, the gas and air mixture speed is fast in the option one.

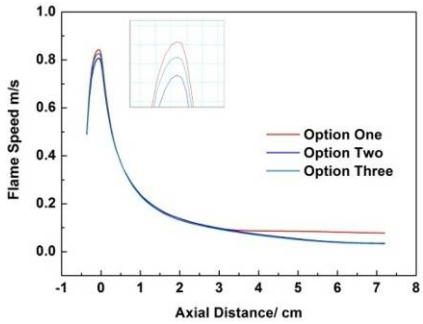

Fig.5 Combustion Velocity Distribution Along the Central Axis

Figure 5 shows that when the jet diffusion of three scenarios is combusting, the distribution of the flame speed along the central axis. As can be seen from Figure 5, when the gas outlet diameter is 0.72cm, outlet speed is 11.4cm/s, the gas combustion speed is 80cm/s or so at the outlet, the speed decreases along the central axis of the outlet, the axial distance in the range of 0~1cm, combustion rate dropps 60cm/s or so, the rate of decline is significant, description gas and air mixes full within this range, combustion reaction speed rapid, flame height develops from the outlet location to the 3.5cm along the central axis, combustion rate decreases, combustion velocity of the three options are basically same, the gas combustion rate is slightly higher along the central axis of option one, when the flames spread is 3.5cm, the gas combustion rate basically unchanged of option one, the gas combustion rate decreased slightly of option two and option three.

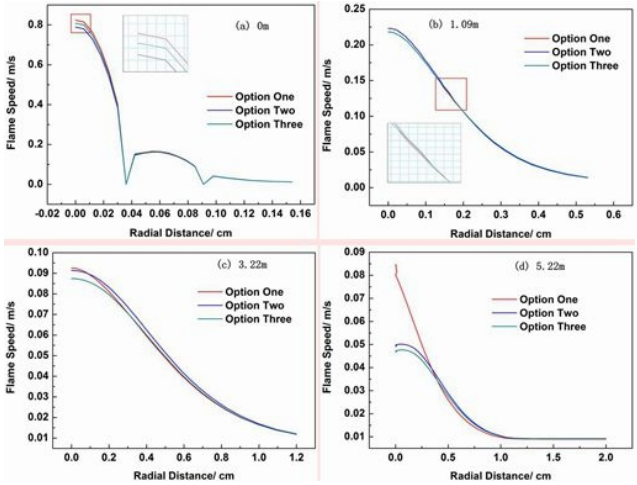

Fig.6 Radial Velocity Distribution at Different Axial Distances

Figure 6 shows that when the gas outlet diameter is 0.72cm, outlet speed is 11.4cm/s, three scenarios jet diffusion combustion, different combustion flame height radial velocity profile, figure (a) is the exit of the radial velocity distribution, figure (b) is 1.09cm of axial distance, figure (c) is 5.25cm of axial distance, figure (d) is 7.20cm of axial distance. As can be seen from figure (a), combustion velocity radius of three option is 0.16cm, combustion velocity is 3 segments distribution, the combustion have the same speed at the outlet, the combustion speed of option one is higher, reaches 82.4cm/s, within a speed radius of 0.04cm range, flame propagation speed decreases, the gas and air are rapid mix, within the range of radius of 0.04~0.085cm, flame velocity distribution curved, the combustion velocity of three programs is basically the same, as can be seen from figure (b), at an axial distance is 1.09cm, the radius of flame speed is 0.6cm, is a monotonically decreasing from radial, combustion velocity of three options are basically the same, as can be seen from figure (c), flame velocity distribution is similar with 1.09cm, when the axial distance is 3.22cm, flame speed is monotonically decreasing from radial, speed radius expanded to 1.2cm, the combustion rate of option two is slightly lower than the other two programs combustion

rate in the vicinity of the axis, as can be seen from figure (d), axial distance is 5.25cm, the combustion rate of three options is monotonically decreasing along radial, equilibrium is reached at a radius of 1cm, in the vicinity of the central axis, option one combustion rate is significantly higher than the burning speed of other programs.

Combustion Temperature Field

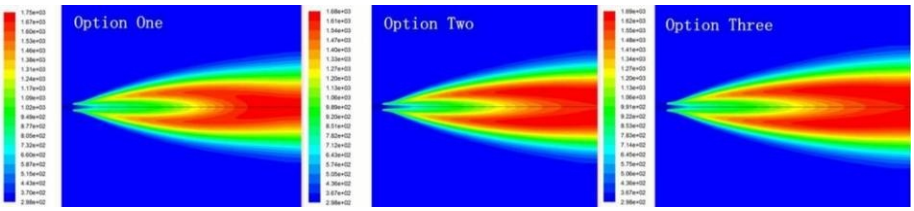

Fig.7 Combustion Temperature Field

Figure 7 shows the different options jet diffusion combustion temperature field. As can be seen from Figure 7, when the gas outlet diameter is 0.72cm, outlet speed is 11.4cm/s, the high temperature zone of combustion is distributed In the flame height is larger than 3cm, flame radius 0.2cm~0.4cm, gas and air well mixed in this region, reaches the flammable range, format an external combustion flame, flame height in the range of 3cm, near the central axis of the jet fire cone, air content is less, gas and air mixture is not sufficient, flame temperature is low, comparison of three combustion temperature field can be seen, the mass fraction of the gas of hydrocarbons is 96% in option one, mass fraction of C and H in the gas is highest, lead to combustion temperature of option one is higher than others, compare with option two and option three combustion temperature field can be seen, the mass fraction of the two solutions close to the gas hydrocarbons, resulting in combustion temperature similar.

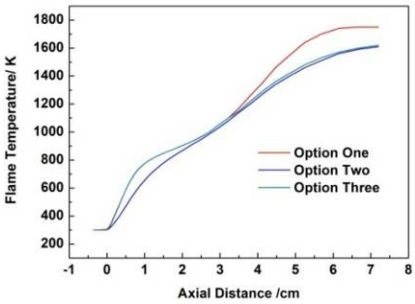

Fig.8 Combustion Temperature Distribution Along the Central Axis

Figure 8 shows that the temperature of jet diffusion flame of three options located in the central axis. As can be seen from Figure 8, when the gas outlet diameter is 0.72cm, outlet speed is 11.4cm/s, the combustion temperatures of jet diffusion flame increase with height increases flame, in the flame at a height of 1cm and 6cm, combustion temperature appears peak, when shale gas of option one is burning, the combustion temperature of central axis is highest, reaches 1750K, when the height of the flame is within 4cm～7cm, combustion temperature is higher than the other two programs 60K ~ 170K, combined with the combustion temperature distribution can be seen, flame height in the range of 4cm ~ 7cm, flame radius of option one decreases, gas and air well mixed, combustion is more complete, flame temperature is higher, central axis of the temperature is relatively option two and option three distribution can be seen, when the flame height at about 1cm, combustion temperature of option two is higher than the combustion temperature of option three, maximum difference is about 140K, with the increase of flame height, combustion temperature of two options is close.

Conclusions

(1) When shale gas and CNG diffusion combustion, the distance along the central axis within the range of 3cm, methane mass fraction decreases significantly, among them, the mass fraction of methane of option one significant decline, when the shale gas of option two and CNG of option three in vehicles diffusion combustion, the distribution of OH radicals in the flame, mainly concentrated in the outer flame region of the flame, option one in shale gas combustion flame OH radicals concentrated at the top.

(2) The diffusion combustion velocity of shale gas of option two and CNG of option three distributions similar, diffusion combustion speed of shale gas of option one is fast, the axial distance is in the range of 1cm, gas and air mixture fastest, resulting in combustion speed decline significant, with height flame increases, combustion speed monotonically decreasing along the radius.

(3) Methane mass fraction of shale gas of option one is highest, reaches 93.5%, jet diffusion flame combustion temperature is higher than the combustion temperature of the other two programs, along the central axis of the flame temperature is gradually increased, the radius of the flame increases, the combustion temperature of the flame height at different radial unmoral distribution.

Acknowledgements

This work was financially supported by National Natural Science Foundation of China(No. 51376083) and College Graduate Research and Innovation Projects in Jiangsu Province Year 2013(No. CXZZ13_0672).

References

[1] U.S.Energy Information Administration. World shale gas resources: An initial assessment of 14 regions outside the United States[M]. 2011,Washington,DC:1-365.

[2] Shale Gas Development Planning(2011-2015)[J].

[3] Gu Xin,Zang Shu-Sheng,et al. Characteristics of Non-Premixed Flame Structure in Humid Air Combustion[J].Journal of Engineering Thermophysics, 2006,27(2):343-346.

[4] Luan Qian-Qian. Numerical Simulation of High Velocity Gas Burner[D].Tianjin University,2007.

[5] Zeng Yi,Fang Jun,Tu Ran,Guan Jin-Fu,Zhang Jun,Zhang Yong-Ming. Variation of Enclosure Fire Ceiling Smoke Concentration with High Altitude[J]. Journal of Combustion Science and Technology, 2011,17(4):332-336.

[6] Zhao Zhen-Xin,Cao Zi-Dong, et al. Study of the Combustion Stability Characteristics of a Direct-flow Type Low-heating-value Coal Gas Burner[J]. Journal of Engineering for Thermal Energy And Power, 2010,25(5):517-520,575-576.

[7] Xiao Xian-Ming,Song Zhi-Guang,Zhu Yan-ming, et al. Summary of shale gas research in North American and revelations to shale gasexploration of Lower Paleozoic strata in China south area[J]. Journal of China Coal Society, 2013,38(5):721-727.

[8] Qiao L, Kim C H, et al.Suppression Effects of Diluents on Laminar Premixed Hydrogen/Oxygen/Nitrogen Flames[J]. Combustion and Flame, 2005, 143(1/2): 79-96.